PLOS ONE

Quantitative CT Variables Enabling Response Prediction in Neoadjuvant Therapy with EGFR-TKIs: Are They Different from Those in Neoadjuvant Concurrent Chemoradiotherapy?

Yousun Chong[1,9], Jae-Hun Kim[1,9], Ho Yun Lee[1]*, Yong Chan Ahn[2], Kyung Soo Lee[1], Myung-Ju Ahn[3], Jhingook Kim[4], Young Mog Shim[4], Joungho Han[5], Yoon-La Choi[5]

1 Department of Radiology and Center for Imaging Science, Sungkyunkwan University School of Medicine, Seoul, Korea, 2 Department of Radiation Oncology, Sungkyunkwan University School of Medicine, Seoul, Korea, 3 Division of Hemato-Oncology, Department of Internal Medicine, Sungkyunkwan University School of Medicine, Seoul, Korea, 4 Department of Thoracic Surgery, Sungkyunkwan University School of Medicine, Seoul, Korea, 5 Department of Pathology, Samsung Medical Center, Sungkyunkwan University School of Medicine, Seoul, Korea

Abstract

Background and Purpose: To correlate changes of various CT parameters after the neoadjuvant treatment in patients with lung adenocarcinoma with pathologic responses, focused on their relationship with different therapeutic options, particularly of EGFR-TKI and concurrent chemoradiation therapy (CCRT) settings.

Materials and Methods: We reviewed pre-operative CT images of primary tumors and surgical specimens obtained after neoadjuvant therapy (TKI, n = 23; CCRT, n = 28) from 51 patients with lung adenocarcinoma. Serial changes in tumor volume, density, mass, skewness/kurtosis, and size-zone variability/intensity variability) were assessed from CT datasets. The changes in CT parameters were correlated with histopathologic responses, and the relationship between CT variables and histopathologic responses was compared between TKI and CCRT groups.

Results: Tumor volume, mass, kurtosis, and skewness were significant predictors of pathologic response in CCRT group in univariate analysis. Using multivariate analysis, kurtosis was found to be independent predictor. In TKI group, intensity variability and size-zone variability were significantly decreased in pathologic responder group. Intensity variability was found to be an independent predictor for pathologic response on multivariate analysis.

Conclusions: Quantitative CT variables including histogram or texture analysis have potential as a predictive tool for response evaluation, and it may better reflect treatment response than standard response criteria based on size changes.

Introduction

Locally advanced non-small cell lung cancer (NSCLC) has a dismal prognosis with a median overall survival (OS) of 25–35 months despite multimodal treatment including radiation therapy (RT), chemotherapy and surgery [1,2]. Induction concurrent chemoradiation therapy (CCRT) is known to result in short-term gross tumor volume reduction, with aggressive locoregional control. Previous studies demonstrated variable responses with volume reduction averaging 38% to 73% [3], with improved survival compared with the treatment of surgery alone [4]. This may be explained by the potent local control effect of irradiation. Therefore, there is a need for studies directed toward predicting treatment benefit versus risk of treatment failure. Clinically, such

predictors would allow further individualization of treatment during radiotherapy [5].

On the other hand, during the last decade, several molecular-targeted agents—for example, epidermal growth factor receptor tyrosine kinase inhibitors (EGFR-TKIs) such as erlotinib and gefitinib—have emerged for treatment of NSCLC [6], as well as in the neoadjuvant setting, which has also shown to be effective in a subset of patients with NSCLC [7–10]. Furthermore, although TKI agents are most active in patients with an EGFR mutation, patients without documented mutation still showed survival benefit compared with placebo [9].

With the advancement in imaging techniques and their increasing application to oncology practice, imaging-based tumor volume regression rate evaluated at mid-RT has been shown to predict local control rate and disease-free survival (DFS) after RT

or CCRT [11,12]. In addition, quantitative measurement of tumor regression rate becomes more realistic with the use of imaging — particularly during therapy when the morphologic changes remain subtle and difficult to assess by clinical examination [12,13]. Evaluation of treatment response to TKI agents is also challenging. It is well established that the conventional RECIST underestimates response rates than the proportion of patients who actually experience clinically effective disease control [7,10,14–20]. Since TKI agents aim for inhibition of tumor cell growth, but not necessarily tumor cell death, tumor response may not emerge as early decrease in tumor size [19]. Very recently, histogram analysis or texture analysis is receiving attention as a method for quantifying tumor heterogeneity and evaluating treatment response [14,21,22].

Here, the question remains which is more effective to predict treatment response in the various imaging-based quantitative assessment methods, and whether or not each method acts differently depending on therapeutic regimen.

Given the need for clinical validation of any updated analysis tool, our main objectives were to identify differences in serial changes of various CT-based parameters in patients with lung adenocarcinoma scheduled to undergo surgical resection after neoadjuvant therapy, and to correlate those changes with pathologic responses, focused on their relationship with different neoadjuvant therapeutic options, particularly of EGFR-TKI and concurrent chemoradiation therapy (CCRT) settings.

Materials and Methods

The institutional review board of Samsung Medical Center (SMC IRB) approved this retrospective study with a waiver of informed consent.

Patients

From September 2005 through December 2011, 398 patients with stage IIIA NSCLC underwent curative surgical resection of lung cancer at our institution, after neoadjuvant treatment (chemotherapy, radiation therapy, or both). Among these patients, patients with pathologically proven adenocarcinoma were only included, while other histologic subtypes (such as squamous cell carcinoma, large cell carcinoma, small cell lung cancer, neuroendocrine cancer, etc.) were excluded. We subdivided the patients into three groups, depending on different neoadjuvant treatment options: chemotherapy with TKI agents, chemotherapy with conventional agents, and CCRT. Since our interest lay in comparing the imaging parameter changes for treatment response prediction between novel TKI and CCRT as a neoadjuvant option, patients who underwent neoadjuvant chemotherapy with conventional agents were excluded. As a result, two groups of patients were enrolled in our study: patients who underwent neoadjuvant chemotherapy with TKI agents, and those who underwent CCRT. Patients for neoadjuvant TKI agent were assembled from a selected population fulfilling $\geq$ two of the following features: female, adenocarcinoma, nonsmoker, and Asian. Regimen of TKI group comprised 1 tablet of 150 mg of erlotinib daily for 3 weeks. Neoadjuvant CCRT included chemotherapy and concurrent thoracic radiotherapy (TRT). The chemotherapy regimen was weekly paclitaxel (50 mg/m^2 per week IV) plus cisplatin (25 mg/m^2 per week IV) or weekly paclitaxel (50 mg/m^2 per week IV) plus carboplatin (AUC 1.5/week IV) for 5 weeks. The concurrent TRT dose was 45 Gy over 5 weeks (1.8 Gy/fraction per day, 5 fractions/week). Surgical resection was planned around 6 weeks after the completion of neoadjuvant therapy for CCRT group, and was scheduled in the fourth week after start of treatment for TKI group. Surgical resection involved a radical resection of the tumor, preferably by lobectomy, and regional lymph node dissection.

Ultimately, 51 patients (25 men and 26 women) satisfied our inclusion criteria. Twenty-three patients received neoadjuvant chemotherapy with TKI, while 28 patients underwent concurrent chemoradiation therapy.

Imaging protocol

In all patients, baseline contrast-enhanced CT before treatment commencement, and follow up contrast-enhanced CT after 4–6 weeks of neoadjuvant treatment were performed.

Image data analysis

A thoracic radiologist (Y.C., with 4 years of experience in thoracic CT interpretation) who was unaware of other patient data evaluated the acquired images semiquantitatively. Only the primary tumors were analyzed. Tumors were segmented by drawing a region of interest (ROI) covering as large an area as possible of the whole tumor. Next, voxel-based CT numbers were collected from lesion segmentations. Since the lesions were segmented to cover the entire tumor, larger lesions had more number of segments than smaller lesions.

For tumor density and volume, the computer automatically calculated the density (g/cm^3) from mean attenuation of total voxels and volume (cm^3) by multiplying the number of voxels by the unit volume of a voxel [23]. Tumor mass (in grams) was calculated by multiplying tumor volume (in cubic centimeters) by mean tumor density [24]. Next, a spreadsheet of all of the values was created, which was used to compute histogram distribution parameters of kurtosis and skewness [25]. The skewness and kurtosis were computed from the segmented tumor region. On histograms, skewness represented the distribution pattern of CT attenuation values; negative and positive skewness indicated that the data were more spread to the left and right of the mean, respectively. Kurtosis represented the position of peak height that indicates CT attenuation value of the maximum number of voxels, with leptokurtic indicated by a sharper peak and platykurtic indicated by a flatter peak (Figure 1).

Texture analysis was performed by a radiology physicist (J.H.K.) with four years of experience in radiology physics. Voxel values within the segmented tumors were resampled to yield 16 of discrete values in order to reduce the noise in image and to normalize the intensity across subjects by clustering voxels with similar intensities [26]. From the discrete tumor images (16 gray levels), the gray level size zone matrix was computed. The value of the matrix's (m, n) is defined by the number of homogenous regions given the homogeneous tumor size (n) to their intensity (m). For example, 'Matrix's (3, 5) is 6.' means that there are 6 homogenous regions, in which the grey level of each cluster is 3, and the size of each cluster is 5 voxels. This gray level size zone matrix was used to compute the variability in the size and the intensity of homogeneous tumor regions [26,27].

Pathologic evaluation of treatment response

Pathologic response was used as the reference standard of therapeutic response. An experienced lung pathologist (J.H. with 20 years of experience in lung pathology) retrospectively interpreted entire tissue sections sliced at 5- to 10-mm intervals and measured the proportion (%) of viable tumor cells in the primary tumor of the resected surgical specimens [28]. Tumor regression was scored as 'pathologic response' if more than 50% necrosis was present with morphologic signs of therapy-induced regression or 'no response' when either 0%–50% necrosis or
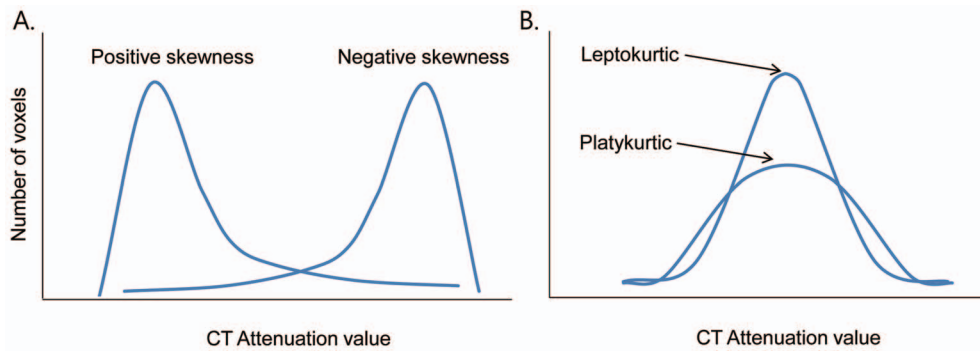
Figure 1. Histogram distributions of CT attenuation value. (a) Skewness. A negative skewness indicates an elongated tail on the left side of the mean, with most values lying to the right of the mean. A positive skewness indicates an elongated tail on the right side of the mean, with most values lying to the left of the mean. (b) Kurtosis. Leptokurtosis indicates a sharper peak, and platykurtosis indicates a flatter peak.
doi:10.1371/journal.pone.0088598.g001

necrosis that could not be attributed to the therapy effect was seen [6]. If more than 90% necrosis was present in the resected specimen, tumor regression was defined as 'near- complete pathologic response' [6].

In addition, comprehensive histologic subtyping was made for the primary tumor in a semi-quantitative manner. Tumors were stratified into the following three grades based on histologically predominant subtypes as: low grade; intermediate grade; and high grade [29,30].

EGFR/KRAS mutational status had been determined by a pathologist (Y.L.C.) by using polymerase chain reaction (PCR) and a direct DNA sequencing method, as previously described [31].

Statistical analysis

Statistical differences between TKI group and CCRT group were analyzed by using either the Mann Whitney test or the Fisher exact test. To identify variables that could be used in differentiating pathologic responders from nonresponders, logistic regression analysis was conducted. Characteristics with a p value of less than 0.50 at univariate analysis were used as the input variables for multiple logistic regression analysis. In multiple logistic regression analysis, a backward stepwise selection mode was used, with iterative entry of variables on the basis of test results ($p < 0.05$). The removal of variables was based on likelihood ratio statistics with a probability of 0.10. ROC analysis was also performed to evaluate the differentiating performance of multiple logistic regression models in discriminating pathologic responders from nonresponders. All analysis was performed using SPSS for Windows, version 12.0 (SPSS, Inc., Chicago, IL).

Results

Baseline characteristics

The TKI group consisted of 23 patients, and the CCRT group included 28 patients. There was a discrepancy in gender distribution and smoking habit, with female predominance(17 out of 23) in the TKI group and male predominance(19 out of 28) in the CCRT group ($p = 0.004$). This was because never smoker females were selected and included in the neoadjuvant TKI treatment planning. Otherwise, all baseline CT and PET features did not show significant difference between the two groups (Table 1). Also, all pathologic and genetic features did not differ significantly in each group.

CT parameters and pathologic response

Percent changes of CT parameters in pathologic responders and pathologic nonresponders were tabulated and compared in both CCRT group and TKI group (Table 2, Figure 2). In case of CCRT group, percent decreases of tumor volume and mass were significantly greater in pathologic responders, as compared with pathologic nonresponders (ps = 0.028 and 0.018, respectively).

As for histogram analysis, in pathologic responders, the lesion showed negative changes in skewness and kurtosis, indicating platykurtosis and negative skewness (Figure 3). Percent changes of kurtosis and skewness were significantly different between pathologic responders and nonresponders in CCRT group (ps = 0.001 and 0.005, respectively), while those were not in TKI group.

On the other hand, in TKI group, intense variability and size-zone variability was significantly decreased in pathologic responders group (ps = 0.005 and 0.003, respectively), as compared with nonresponders (Figure 3). These significant differences were not found in CCRT group. Decrease in intense variability and size-zone variability reflects homogeneous change of vascularity [14,26].

Logistic Regression Analysis and ROC Analysis

In TKI group, intense variability and size-zone variability were used as input variables for multivariate logistic regression analysis. Multivariate analysis disclosed that intense variability was the sole significant predictor of pathologic response ($p = 0.028$; 95% confidence interval: 1.009, 1.184; adjusted odds ratio, 1.093) (Table 3). ROC analysis showed that the area under the ROC curve (AUC) for intense variability was 0.931 and that the optimal cut-off value of percent change of intense variability for predicting pathologic response was less than –6.9 (sensitivity, 92.3%; specificity, 80%).

In CCRT group, tumor volume, mass, kurtosis, and skewness were used as input variables for multivariate logistic regression analysis. Multivariate analysis displayed that kurtosis was the sole significant predictor of pathologic response ($p = 0.009$; 95% confidence interval: 1.026, 1.195; adjusted odds ratio, 1.107) (Table 3). ROC analysis showed that the AUC for kurtosis was 0.943 and that the optimal cut-off value of percent change of kurtosis for predicting pathologic response was less than –23 (sensitivity, 87.5%; specificity, 84.3%).

Discussion

Our study showed various imaging-based quantitative assessment methods worked differently with different therapeutic

Table 1. Clinicopathologic and baseline radiologic characteristics according to the neoadjuvant regimen.

	TKI group	CCRT group	
	(n = 23)	(n = 28)	P values
Age (y)**	55.6±9.1	56.5±10.5	.732
Gender			.004*
Male	6 (26)	19 (68)	
Female	17 (74)	9 (32)	
Smoking habit			<.001*
Never	22 (96)	14 (50)	
Ever	1 (4)	14 (50)	
Histology type			
Adenocarcinoma	23 (100)	28 (100)	1.00
Stage			
IIIA	23 (100)	28 (100)	1.00
Baseline CT features			
Volume (cm³)	22.7±23.8	31.9±47.8	.405
Density	1.13±0.51	1.14±0.34	.458
Mass (g)	25.9±28.1	36.6±55.2	.403
Histogram Analysis			
Kurtosis	35.5±87.5	17.2±11.9	.280
Skewness	−1.91±4.58	−2.42±1.99	.600
Texture Analysis			
Intensity variability	8.00±3.83	6.87± 4.42	.338
Size-zone variability	23.5±10.8	22.7±18.6	.857
Baseline PET features			
SUVmax**	10.3±3.8	12.7±6.5	.180
Pathologic features			
Response			.924
Responder[+]	10 (43)	12 (43)	
Near complete responder[++]	4 (17)	7 (25)	
Nonresponder	13 (57)	16 (57)	
Differentiation			.066
Well-	1 (4)	0 (0)	
Moderately-	21 (92)	21 (75)	
Poorly-	1 (4)	7 (25)	
EGFR mutation			.721
Positive	11 (48)	5 (18)	
Negative	10 (43)	6 (21)	
Unknown	2 (9)	17 (61)	
KRAS mutation			.467
Positive	0 (0)	2 (7)	
Negative	7 (30)	6 (21)	
Unknown	16 (70)	20 (72)	

TKI, tyrosine kinase inhibitors; CCRT, concurrent chemoradiation therapy.
Note.—Unless otherwise indicated, data in parentheses are percentages.
* P <.05.
** Data are the range.
[+]Less than 50% of viable tumor cells in the resected specimen.
[++]Less than 10% of viable tumor cells in the resected specimen.
doi:10.1371/journal.pone.0088598.t001

regimens, particularly of EGFR-TKI setting and CCRT setting. We found tumor volume, mass, kurtosis, and skewness were all significant predictors of pathologic response in CCRT group in univariate analysis. Using multivariate analysis, kurtosis was found to be independent predictor. On the other hand, in TKI group, heterogeneity from texture analysis was an independent predictor for pathologic response. Our results suggest the possible value of adapting various combination of imaging parameters for response evaluation beyond size-based measurement according to the different treatment modality used. Since there is raising request for personalized and optimized therapy, an advanced diagnostic tool to predict treatment response more accurately is required.

Prognostic factors are an essential requirement in the management of NSCLC and this is reflected in recent changes in the TNM staging [32], where each sub-group is indicative of outcome. However, despite such refinements, there remains uncertainty and more predictive data are required. This is particularly true in Stage 3A disease where outcome remains variable [33]. Moreover, the selection and benefit of surgical patients for neo-adjuvant/adjuvant treatment is also unclear [34,35]. It is important that the possible survival benefits of chemoradiation should be balanced by the adverse effects of toxicity to the patient [36]. Through the early identification of patients who will not get a clinical benefit from treatment, patients could be saved from drug toxicity and they could be switched to an alternative treatment earlier. Moreover, there are potential cost savings if drugs are used in only those patients who will benefit from them [14]. Recent additional option of targeted agents makes the situation more complicated. Imaging-defined response assessment (RECIST) is a cornerstone of modern oncologic practice; however, it is limited in a number of targeted therapies, including treatment with TKIs. In a recent study evaluating tumor response to neoadjuvant erlotinib in 60 patients with NSCLC, radiologic response by RECIST was observed in only 5% of the patients, while pathologic response was shown in 23% of the patients [10]. Furthermore, as our figure 2A, the ground-glass opacity component of the tumor may remain at the exact area of pretreatment solid component of the tumor, where volume reduction of the lesion is not significant [19], Therefore, even near complete pathologic response was not predicted by CT-driven RECIST, suggesting that RECIST was suboptimal for short-term radiologic response evaluation. This is because apoptosis, transition of necrosis to fibrosis, or lymphocytic and granulomatous reactions may not result in early decrease in tumor size [10]. These results support the need for development of an optimal imaging parameter for early response evaluation and accurate prediction. In that regard, quantitative CT analysis may be emerging as a potential tool for doing this task.

In the CCRT group, volume decrease was significantly greater in the pathologic responder group, with mean volume reduction of 56.4%. Early volume decrease is achieved by potent locoregional control with cytotoxic effect of irradiation. Volume reduction rate in our study correlates with the results of previous studies [3].

Moreover, skewness and kurtosis could predict pathologic response in the CCRT group. Two values all decreased greater in the pathologic responders, as compared in the nonresponders. Decreased skewness or positive skewness reflects decreased enhancement, which may result from decreased neovascularization.

Meanwhile, CT variables reflecting tumoral heterogeneity were significant prognostic factors for pathologic response in TKI group. A previous study assessing tumor heterogeneity using CT texture in NSCLC patients reported poorer survival in patients who had heterogeneous tumors with low uniformity values [21]. In addition, Tixier et al. analyzed textural features on FDG-PET

Table 2. Percent changes of CT parameters in relation to pathologic response.

CT parameters	TKI group (n = 23)			CCRT group (n = 28)		
	Pathologic responder	Pathologic nonresponder		Pathologic responder	Pathologic nonresponder	
	(n = 10)	(n = 13)	P values	(n = 12)	(n = 16)	P values
%Volume (cm^3)	−51.5±28.1	−42.5±21.7	.266	−56.4±42.2	−14.3±42.5	**.028***
%Density	−9.5±12.5	−5.1±9.7	.349	−8.5±11.8	−5.1±12.1	.209
%Mass (g)	−56.9±23.7	−40.0±31.9	.095	−61.8±36.2	−17.9±43.7	**.018***
Histogram Analysis						
%Kurtosis	−27.7±47.8	−18.4±36.9	.605	−48.0±23.1	1.7±38.6	**.001***
%Skewness	−26.8±39.8	−22.4±29.1	.760	−34.2±28.9	−1.7±26.9	**.005***
Texture Analysis						
%Intensity variability	−35.3±31.3	21.6±50.7	**.005***	92.1±33.3	60.4±81.5	.689
%Size-zone variability	−50.2±23.7	−1.3±40.9	**.003***	−32.9±21.5	−28.0±32.6	.652

TKI, tyrosine kinase inhibitors; CCRT, concurrent chemoradiation therapy.
Note.—Data are mean ± standard deviation of the percent change n the given parameter.
* P <.05.
doi:10.1371/journal.pone.0088598.t002

images in patients with esophageal cancer who underwent concomitant chemoradiation therapy, and found textural features can predict responders (complete and partial) better than can SUV [26]. In their study regional tumor heterogeneity represented by intensity and size-zone variability was a significant predictor of response, rather than global measurement including SUV. Similar results were found in our study, in which intensity variability was a significant independent predictor for pathologic response in patients treated with neoadjuvant TKI agents. Significantly decreased intensity variability and size-zone variability in the pathologic responder group reflects increased tumoral homogeneity, including homogeneous change of vascularity. However, these texture parameters were not helpful in predicting response in the CCRT group. Such reasoning may be explained in part by the difference in pharmagophysiologic reactions according different treatment regimens.
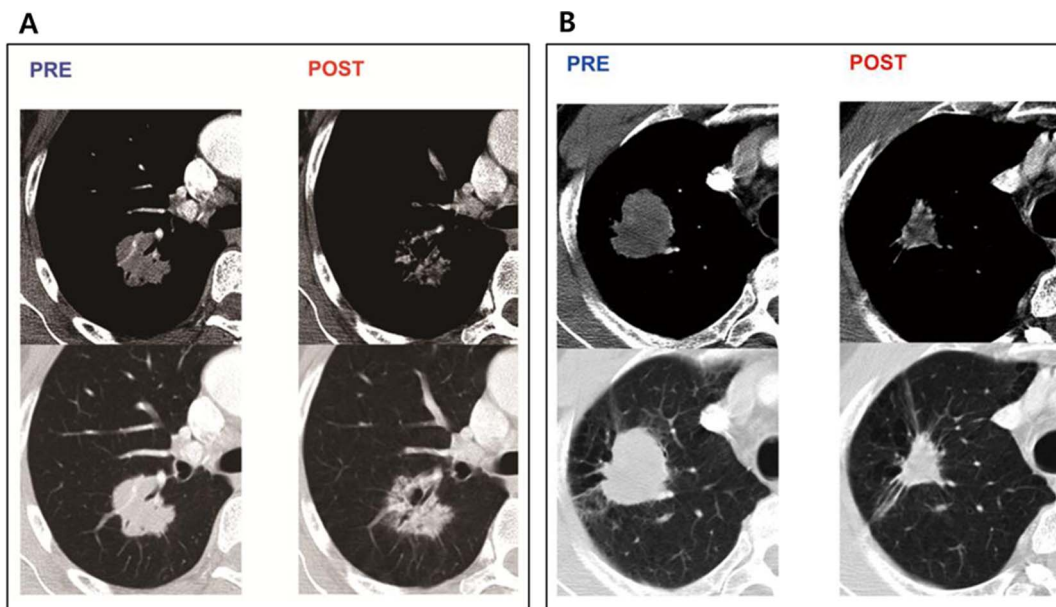

Figure 2. Quantitative CT parameters of pathologic responder. (a) Combined histogram distributions of the treatment before (blue) and after (red). As for histogram distribution, the vertical axis in each histogram shows the number of pixels in the segmented tumor. The horizontal axis shows the CT attenuation values. Attenuation value is shifted to the left from the blue to the red graph. (b) Intensity size-zone matrix of the treatment before (blue) and after (red). The horizontal axis shows size of homogenous area. Divergent distribution on the horizontal axis indicates increased size-zone variability. The vertical axis shows intensity. Divergent distribution on the vertical axis indicates increased intensity variability. Distributions of the points on the matrix become more convergent and clustered both in the horizontal axis and the vertical axis from the pre-treatment matrix to the post-treatment matrix.
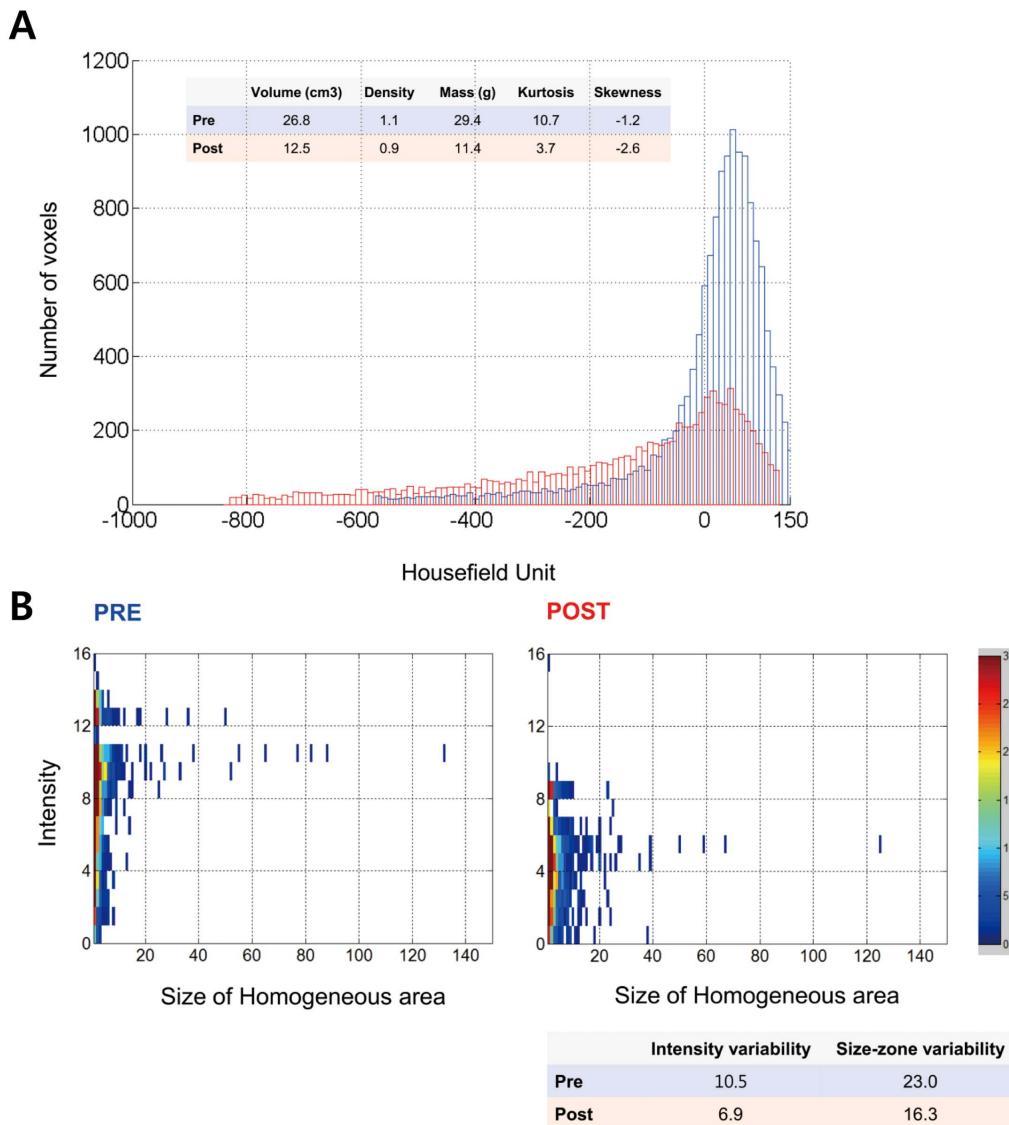doi:10.1371/journal.pone.0088598.g002

A

	Volume (cm3)	Density	Mass (g)	Kurtosis	Skewness
Pre	26.8	1.1	29.4	10.7	-1.2
Post	12.5	0.9	11.4	3.7	-2.6

B

PRE

POST

	Intensity variability	Size-zone variability
Pre	10.5	23.0
Post	6.9	16.3

Figure 3. CT images of TKI group and CCRT group. (a) A 56-year-old woman with lung adenocarcinoma who underwent neoadjuvant treatment with EGFR-TKI. Pretreatment CT scans on mediastinal and lung window images show a lobulating sold mass. CT scans obtained after treatment show that the ground-glass opacity component of lesion is remaining on lung window image at the exact area of pretreatment solid component, and reduction of the lesion extent is not significant, (b) A 68-year-old man with lung adenocarcinoma who underwent neoadjuvant treatment with CCRT. Pretreatment CT scans on mediastinal and lung window images show a lobulating sold mass. CT scans obtained after treatment show significant volume reduction of the tumor.
doi:10.1371/journal.pone.0088598.g003

Some authors explain potential significance of tumoral heterogeneity by correlation with genomic heterogeneity [36]. It has recently been shown that a genomic heterogeneity exists within tumors, and this observation has significant implications for Darwinist theories of tumor resistance [37]. Whether textural heterogeneity on imaging relates to underlying genomics would be important to investigate. Given the challenges and expense of measuring tumor genomic signatures, then imaging may be more viable option. Another possible meaning is the possible relationship between tumor heterogeneity and hypoxia. It has been recently shown that tumor textural analysis was associated with tumor hypoxia on histological examinations from NSCLC patients who were administered intravenous pimonidazole prior to surgery [38]. Hypoxia is a recognized marker of poor outcome, and as such, a positive relationship between tumor hypoxia and tumor

heterogeneity would be biologically consistent. Additional potential merit of texture analysis is that texture methods can quantify the spatial variations in parametric maps, not the absolute values of the maps. Therefore, texture analysis can provide additional and independent information compared to histogram-based measures of parametric maps [39].

A potential limitation of our study is its retrospective design. However, the majority of baseline characteristics did not differ between the two study populations. Even though there was considerable difference in gender distribution and smoking habit, this occurred because never smoker females were enrolled in the neoadjuvant TKI agent treatment arm, in the clinical setting. A relatively small number of patients were included in our study. Further studies with a larger sample size are necessary for validation of our results. Since tumor regions of interest (ROI)

Table 3. Logistic regression analysis of CT variables for predicting pathologic response.

	Variables	Odds ratio	95% CI	P value
TKI group	Intensity variability	**1.093**	**1.009, 1.184**	**0.028**
	Size-zone variability	1.026	0.980, 1.075	0.270
CCRT group	Tumor volume (cm³)	1.188	0.441, 3.202	0.733
	Tumor mass (g)	0.855	0.320, 2.286	0.756
	Kurtosis	**1.092**	**1.028, 1.160**	**0.004**
	Skewness	1.001	0.919, 1.090	0.982

TKI, tyrosine kinase inhibitors; CCRT, concurrent chemoradiation therapy; AUC, area under the curve; CI, confidence interval.
doi:10.1371/journal.pone.0088598.t003

were drawn manually by a single operator, inter- and intra-observer variation may be present. Assistance of an automated software tool could improve this limitation, and furthermore help decrease the time consumed in the tedious work. Despite

limitations in our study, it presented novel methodologies that went beyond the traditional size-based analytical method, to evaluate treatment outcomes in NSCLC patients. Our study provides a proof-of-concept that a multiparametric image-feature-based approach holds promise in planning individualized treatment, and that prospective clinical trials may be warranted to better understand the extent of this approach [5].

In conclusion, quantitative CT variables including histogram analysis or texture analysis has potential as a predictive biomarker, and it may better reflect treatment response than standard response criteria based on size change. Also, different combinations of imaging parameters may be correlated to physiologic processes occurring after various different treatment modalities.

Supporting Information

File S1
(DOCX)

Author Contributions

Conceived and designed the experiments: YC JHK HYL. Performed the experiments: JHK KSL YCA MJA JK YMS JH YLC. Analyzed the data: YC JHK. Contributed reagents/materials/analysis tools: JHK YLC. Wrote the paper: YC JHK HYL KSL YCA MJA JK YMS JH YLC.

References

1. Ahn HK, Choi YL, Han JH, Ahn YC, Kim K, et al. (2013) Epidermal growth factor receptor mutation and treatment outcome of mediastinoscopic N2 positive non-small cell lung cancer patients treated with neoadjuvant chemoradiotherapy followed by surgery. Lung Cancer 79: 300–306.
2. Park BB, Park JO, Kim H, Ahn YC, Choi YS, et al. (2006) Is trimodality approach better then bimodality in stage IIIA, N2 positive non-small cell lung cancer? Lung Cancer 53: 323–330.
3. Kozak MM, Murphy JD, Schipper ML, Donington JS, Zhou L, et al. (2011) Tumor volume as a potential imaging-based risk-stratification factor in trimodality therapy for locally advanced non-small cell lung cancer. J Thorac Oncol 6: 920–926.
4. Katakami N, Tada H, Mitsudomi T, Kudoh S, Senba H, et al. (2012) A phase 3 study of induction treatment with concurrent chemoradiotherapy versus chemotherapy before surgery in patients with pathologically confirmed N2 stage IIIA nonsmall cell lung cancer (WJTOG9903). Cancer 118: 6126–6135.
5. Vaidya M, Creach KM, Frye J, Dehdashti F, Bradley JD, et al. (2012) Combined PET/CT image characteristics for radiotherapy tumor response in lung cancer. Radiother Oncol 102: 239–245.
6. Aukema TS, Kappers I, Olmos RA, Codrington HE, van Tinteren H, et al. (2010) Is 18F-FDG PET/CT useful for the early prediction of histopathologic response to neoadjuvant erlotinib in patients with non-small cell lung cancer? J Nucl Med 51: 1344–1348.
7. Dingemans AM, de Langen AJ, van den Boogaart V, Marcus JT, Backes WH, et al. (2011) First-line erlotinib and bevacizumab in patients with locally advanced and/or metastatic non-small-cell lung cancer: a phase II study including molecular imaging. Ann Oncol 22: 559–566.
8. Sunaga N, Tomizawa Y, Yanagitani N, Iijima H, Kaira K, et al. (2007) Phase II prospective study of the efficacy of gefitinib for the treatment of stage III/IV non-small cell lung cancer with EGFR mutations, irrespective of previous chemotherapy. Lung Cancer 56: 383–389.
9. O'Brien ME, Myerson JS, Coward JI, Puglisi M, Trani L, et al. (2012) A phase II study of (1)(8)F-fluorodeoxyglucose PET-CT in non-small cell lung cancer patients receiving erlotinib (Tarceva); objective and symptomatic responses at 6 and 12 weeks. Eur J Cancer 48: 68–74.
10. Schaake EE, Kappers I, Codrington HE, Valdes Olmos RA, Teertstra HJ, et al. (2012) Tumor response and toxicity of neoadjuvant erlotinib in patients with early-stage non-small-cell lung cancer. J Clin Oncol 30: 2731–2738.
11. Johnson CR, Thames HD, Huang DT, Schmidt-Ullrich RK (1995) The tumor volume and clonogen number relationship: tumor control predictions based upon tumor volume estimates derived from computed tomography. Int J Radiat Oncol Biol Phys 33: 281–287.
12. Mayr NA, Taoka T, Yuh WT, Denning LM, Zhen WK, et al. (2002) Method and timing of tumor volume measurement for outcome prediction in cervical cancer using magnetic resonance imaging. Int J Radiat Oncol Biol Phys 52: 14–22.
13. Hong JH, Chen MS, Lin FJ, Tang SG (1992) Prognostic assessment of tumor regression after external irradiation for cervical cancer. Int J Radiat Oncol Biol Phys 22: 913–917.
14. Goh V, Ganeshan B, Nathan P, Juttla JK, Vinayan A, et al. (2011) Assessment of response to tyrosine kinase inhibitors in metastatic renal cell cancer: CT texture as a predictive biomarker. Radiology 261: 165–171.
15. Shim JH, Lee HC, Kim SO, Shin YM, Kim KM, et al. (2012) Which response criteria best help predict survival of patients with hepatocellular carcinoma following chemoembolization? A validation study of old and new models. Radiology 262: 708–718.
16. William WN, Jr., Pataer A, Kalhor N, Correa AM, Rice DC, et al. (2013) Computed tomography RECIST assessment of histopathologic response and prediction of survival in patients with resectable non-small-cell lung cancer after neoadjuvant chemotherapy. J Thorac Oncol 8: 222–228.
17. Zhao B, Oxnard GR, Moskowitz CS, Kris MG, Pao W, et al. (2010) A pilot study of volume measurement as a method of tumor response evaluation to aid biomarker development. Clin Cancer Res 16: 4647–4653.
18. Kang H, Lee HY, Lee KS, Kim JH (2012) Imaging-based tumor treatment response evaluation: review of conventional, new, and emerging concepts. Korean J Radiol 13: 371–390.
19. Lee HY, Lee KS, Ahn MJ, Hwang HS, Lee JW, et al. (2011) New CT response criteria in non-small cell lung cancer: proposal and application in EGFR tyrosine kinase inhibitor therapy. Lung Cancer 73: 63–69.
20. Lee HY, Lee KS, Hwang HS, Lee JW, Ahn MJ, et al. (2010) Molecularly targeted therapy using bevacizumab for non-small cell lung cancer: a pilot study for the new CT response criteria. Korean J Radiol 11: 618–626.
21. Ganeshan B, Panayiotou E, Burnand K, Dizdarevic S, Miles K (2012) Tumour heterogeneity in non-small cell lung carcinoma assessed by CT texture analysis: a potential marker of survival. Eur Radiol 22: 796–802.
22. Baek HJ, Kim HS, Kim N, Choi YJ, Kim YJ (2012) Percent change of perfusion skewness and kurtosis: a potential imaging biomarker for early treatment response in patients with newly diagnosed glioblastomas. Radiology 264: 834–843.
23. de Hoop B, Gietema H, van de Vorst S, Murphy K, van Klaveren RJ, et al. (2010) Pulmonary ground-glass nodules: increase in mass as an early indicator of growth. Radiology 255: 199–206.
24. Lee HY, Jeong JY, Lee KS, Kim HJ, Han J, et al. (2012) Solitary pulmonary nodular lung adenocarcinoma: correlation of histopathologic scoring and patient survival with imaging biomarkers. Radiology 264: 884–893.
25. Chandarana H, Rosenkrantz AB, Mussi TC, Kim S, Ahmad AA, et al. (2012) Histogram analysis of whole-lesion enhancement in differentiating clear cell from papillary subtype of renal cell cancer. Radiology 265: 790–798.
26. Tixier F, Le Rest CC, Hatt M, Albarghach N, Pradier O, et al. (2011) Intratumor heterogeneity characterized by textural features on baseline 18F-FDG PET images predicts response to concomitant radiochemotherapy in esophageal cancer. J Nucl Med 52: 369–378.
27. Thibault G, Fertil B, Navarro C, Pereira S, Cau P, et al. (2009) Texture indexes and gray level size zone matrix: application to cell nuclei classification. Pattern Recognition Inf Process: 140–145.
28. Lee HY, Lee HJ, Kim YT, Kang CH, Jang BG, et al. (2010) Value of combined interpretation of computed tomography response and positron emission

tomography response for prediction of prognosis after neoadjuvant chemotherapy in non-small cell lung cancer. J Thorac Oncol 5: 497–503.

29. Kadota K, Colovos C, Suzuki K, Rizk NP, Dunphy MP, et al. (2012) FDG-PET SUVmax combined with IASLC/ATS/ERS histologic classification improves the prognostic stratification of patients with stage I lung adenocarcinoma. Ann Surg Oncol 19: 3598–3605.

30. Lee HY, Jeong JY, Lee KS, Yi CA, Kim BT, et al. (2013) Histopathology of Lung Adenocarcinoma Based on New IASLC/ATS/ERS Classification: Prognostic Stratification With Functional and Metabolic Imaging Biomarkers. J Magn Reson Imaging.

31. Yoon HJ, Lee HY, Lee KS, Choi YL, Ahn MJ, et al. (2012) Repeat biopsy for mutational analysis of non-small cell lung cancers resistant to previous chemotherapy: adequacy and complications. Radiology 265: 939–948.

32. Edge SB, Byrd DR, Compton CC, Fritz AG, Greene FL, et al. (2010) AJCC Cancer Staging Manual New York, NY: Springer.

33. Brunelli A, Charloux A, Bolliger CT, Rocco G, Sculier JP, et al. (2009) ERS/ESTS clinical guidelines on fitness for radical therapy in lung cancer patients (surgery and chemo-radiotherapy). Eur Respir J 34: 17–41.

34. Kamal NS, Soria JC, Mendiboure J, Planchard D, Olaussen KA, et al. (2010) MutS homologue 2 and the long-term benefit of adjuvant chemotherapy in lung cancer. Clin Cancer Res 16: 1206–1215.

35. Waller D, Peake MD, Stephens RJ, Gower NH, Milroy R, et al. (2004) Chemotherapy for patients with non-small cell lung cancer: the surgical setting of the Big Lung Trial. Eur J Cardiothorac Surg 26: 173–182.

36. Win T, Miles K, Janes SM, Ganeshan B, Shastry M, et al. (2013) Tumor Heterogeneity as measured on the CT component of PET/CT Predicts Survival in Patients with Potentially Curable Non-Small Cell Lung Cancer. Clin Cancer Res.

37. Gerlinger M, Rowan AJ, Horswell S, Larkin J, Endesfelder D, et al. (2012) Intratumor heterogeneity and branched evolution revealed by multiregion sequencing. N Engl J Med 366: 883–892.

38. Ganeshan B, Goh V, Mandeville HC, Ng QS, Hoskin PJ, et al. (2013) Non-small cell lung cancer: histopathologic correlates for texture parameters at CT. Radiology 266: 326–336.

39. Alic L, van Vliet M, van Dijke CF, Eggermont AM, Veenland JF, et al. (2011) Heterogeneity in DCE-MRI parametric maps: a biomarker for treatment response? Phys Med Biol 56: 1601–1616.